REPORT DOCUMENTATION PAGE

AFRL-SR-BL-TR-00-
0349

1. AGENCY USE ONLY *(Leave blank)*	2. REPORT DATE	3. REPORT TYPE AND DATES COVERED
	July 2000	Final Technical (07/01/96-07/31/99)

4. TITLE AND SUBTITLE
"Uncooled RF Electronics for Airborne Radar"

5. FUNDING NUMBERS
F49620-96-1-0398

6. AUTHOR(S)
Dr. Umesh K. Mishra

7. PERFORMING ORGANIZATION NAME(S) AND ADDRESS(ES)
University of California, Santa Barbara, CA 93106

8. PERFORMING ORGANIZATION REPORT NUMBER

9. SPONSORING/MONITORING AGENCY NAME(S) AND ADDRESS(ES)
AFOSR/NE
801 North Randolph Street, Rm. 732
Arlington, VA 22203-1977

10. SPONSORING/MONITORING AGENCY REPORT NUMBER
F49620-96-1-0398

11. SUPPLEMENTARY NOTES

12a. DISTRIBUTION/AVAILABILITY STATEMENT
Distribution Unlimited, approved for public release.

12b. DISTRIBUTION CODE

13. ABSTRACT *(Maximum 200 words)*

Using MBE efforts, concentration was focused on the homoepitaxial growth of HEMT nitride-based structures on high quality MOCVD templates grown on (0001) sapphire substrates, allowing the avoidance of the sapphire nucleation step, and thus the high dislocation and extended defect density that can occur with direct MBE growth on sapphire.

20000804 200

14. SUBJECT TERMS
MBE, homoepitaxial growth, AlGaN/GaN structures

15. NUMBER OF PAGES
11

16. PRICE CODE

17. SECURITY CLASSIFICATION OF REPORT	18. SECURITY CLASSIFICATION OF THIS PAGE	19. SECURITY CLASSIFICATION OF ABSTRACT	20. LIMITATION OF ABSTRACT
UNCLASSIFIED	UNCLASSIFIED	UNCLASSIFIED	UL

AlGaN/GaN HEMT structure development by MBE

In our MBE efforts, we have concentrated on the homoepitaxial growth of nitride-based structures on high quality MOCVD templates grown on (0001) sapphire substrates. This approach allows one to avoid the sapphire nucleation step and thus the high dislocation and extended defect density that can occur with direct MBE growth on sapphire.

The MBE growth was performed in a Varian Gen II MBE system. Active nitrogen for growth was supplied by a water-cooled EPI Unibulb Nitrogen Plasma source utilizing ultrahigh purity nitrogen (99.9995% purity) which was further purified by an inert gas purifier at the RF-plasma source gas inlet. Elemental Ga (7N) and Al (6N) supplied from conventional effusion cells were used for the group III sources. The system had a base pressure in the mid 10^{-11} torr range with no detectable arsenic or oxygen. This combination of high quality MOCVD templates, an oxygen and arsenic free atmosphere, new generation RF nitrogen plasma sources, high gas purity, and careful studies of the growth mechanisms performed at UCSB in the previous years allowed us to achieve the high quality AlGaN/GaN 2DEG structures.

In order to fully realize the potential of AlGaN/GaN structures, the key mechanisms controlling the formation of the 2DEG at the AlGaN/GaN interface and its properties must be well understood. Therefore in the process of AlGaN/GaN HEMT structure optimization a careful systematic experimental study of the charge transfer and electron transport in this system was conducted. A series of growths was performed on unintentionally doped n-GaN templates produced by atmospheric pressure MOCVD. The MBE grown films consisted of 0.25 - 0.3 μm thick GaN layers followed by $Al_xGa_{1-x}N$ layers of different thicknesses (3 nm < d < 50 nm) and alloy compositions (0.09 < x <

0.31). To eliminate the effect of the parallel conduction through the template during the structure analysis, Van der Pauw Hall effect measurements were performed over the large temperature range including cryogenic temperatures.

The AlGaN barrier thickness study was performed for the Al mole fraction of x = 0.27. It was found that the formation of the 2D electron channel in the unintentionally doped $Al_{0.27}Ga_{0.73}N$/GaN structure occurs starting at a barrier thickness of ~ 3 nm, determined by the energy position of the surface donor-like states. We believe these surface donor-like states act as the source of both the 2DEG electrons and the positive charges compensating the negative polarization-induced charge at the top of the AlGaN layer. Further increase of the barrier width lead to an increase in the number of the 2D electrons and its subsequent saturation at a value close to the value of the polarization-induced charge density in the AlGaN layer (Fig.1a). The variation of the Al content in the AlGaN barrier resulted in an approximately linear change in the 2DEG density at a rate of $dN_s/dx = 5.45 \times 10^{13}$ cm^{-2} (Fig.1b).

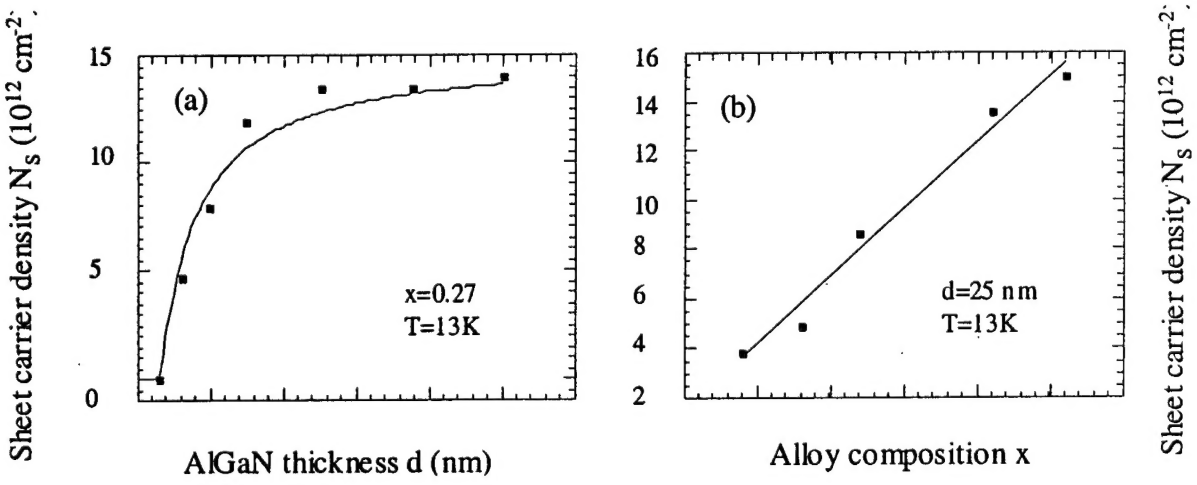

Figure 1. (a) 2DEG sheet carrier density in the $Al_{0.27}Ga_{0.73}N$/GaN structures as a function of AlGaN barrier width. The solid line represents a least square theoretical fit to experimental data [1]; (b) 2DEG sheet carrier density in the $Al_xGa_{1-x}N$/GaN structures as a function of AlGaN barrier composition x. The thin solid line represents a least square linear fit to experimental data.

The high quality of the MBE grown AlGaN/GaN heterostructures was manifested by an extremely high values of the low-temperature electron mobility (Fig.2a,b). The electron mobility of the AlGaN/GaN heterostructures was found to gradually decrease with an increase in both Al mole fraction and thickness of the AlGaN barrier. These experimental results completely rule out the ionized impurity scattering as the main scattering mechanism and may be related to the change in the alloy disorder scattering or interface roughness scattering that significantly intensify as the density of the 2DEG increases.

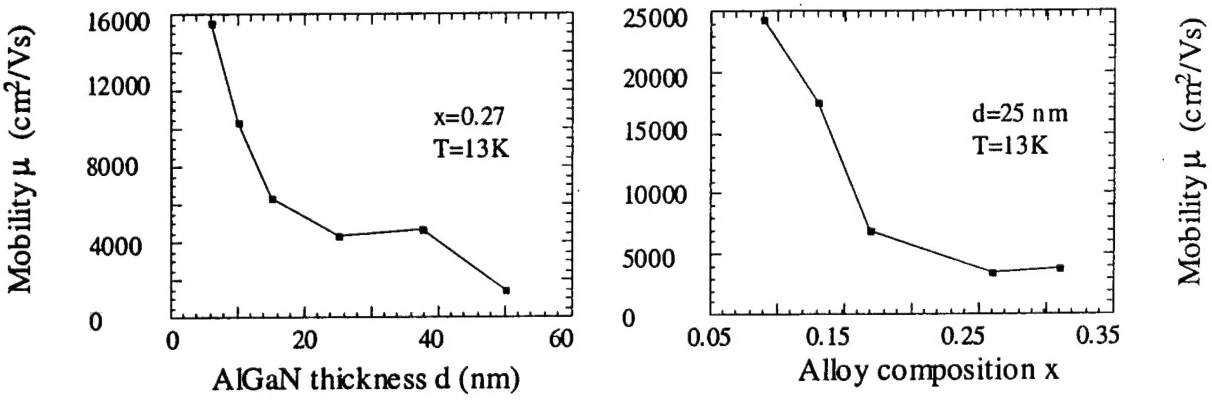

Figure 2. (a) Low-temperature electron mobility in the $Al_{0.27}Ga_{0.73}N$/GaN heterostructures as a function of AlGaN barrier thickness; (b) Low-temperature electron mobility in the $Al_xGa_{1-x}N$/GaN 2DEG structures as a function of alloy composition x.

Based on the empirically established dependences of the electron mobility on AlGaN barrier composition and width we managed to achieve a record low-temperature mobility by utilizing low values of *x* and *d*. The temperature dependence of the electron mobility and the sheet carrier density in the structure with a 16 nm $Al_{0.09}Ga_{0.91}N$ barrier is shown in Figure 3. At 77 K the mobility of this structure was 24,000 cm^2/Vs (N_s (77 K) = 2.5 x 10^{12} cm^{-2}) while at 13 K it reached the value of 51,700 cm^2/Vs (N_s (13 K) = 2.23 x

10^{12} cm^{-2}). To the best of our knowledge, these values of the low-temperature mobility are the highest ever reported in the literature for the AlGaN/GaN system.

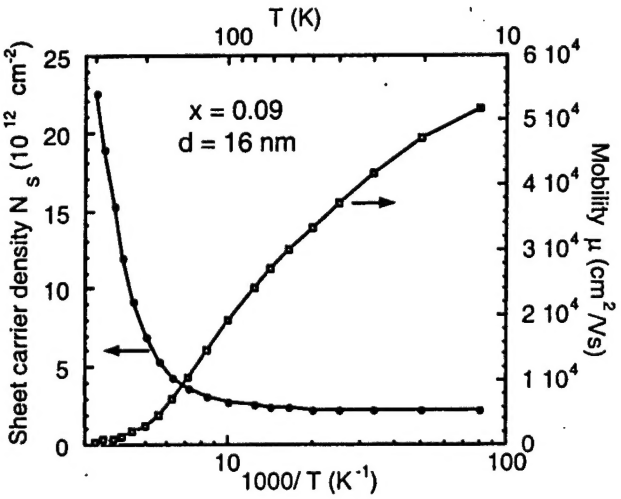

Figure 3. Temperature dependence of the Hall mobility and the sheet carrier concentration in the $Al_{0.09}Ga_{0.91}N$/GaN heterostructure with 16 nm AlGaN barrier.

High Power HFETs by MBE

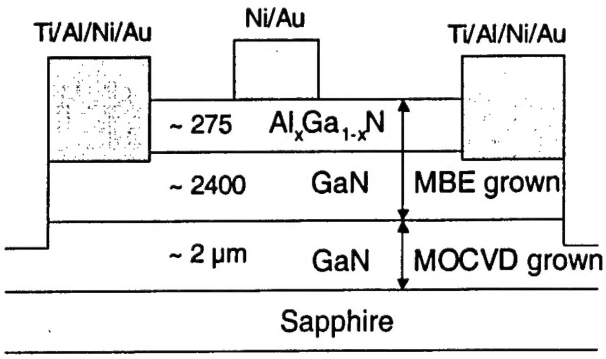

Fig 4. The layer structure of the device.

The device layers were grown on a 2 μm semi-insulating GaN template grown by MOCVD on c-plane sapphire. On the GaN template, approximately 2400 Å of unintentionally doped GaN, followed by 275 Å of unintentionally doped $Al_{0.25}Ga_{0.75}N$ was grown by MBE. Room temperature Hall measurements yielded a sheet carrier concentration of 1.45 x $10^{13}/cm^2$ and a Hall mobility of 1290 cm^2/Vs. Device fabrication began with deposition of source/drain ohmic contacts (Ti/Al/Ni/Au) which were annealed at 880°C. Ni/Au/Ni was used for the gate Schottky contact. Mesa isolation was achieved by reactive ion etching.

Results: Typical I-V characteristics are shown in Fig 5. The maximum drain current I_{MAX} obtained at a positive gate bias of +2 V was 1050 mA/mm. However the ohmic contact resistance of 4 Ω.mm is still significantly higher than the value of 0.5 Ω.mm reported in [4] and further optimization is necessary. For a gate drain spacing of 1μm, DC breakdown voltages were ~50 V. Measured unity current gain cutoff frequency f_t and unity power gain cutoff frequency f_{max} were 17.5 GHz and 33 GHz respectively for a device with a gate length (L_g) of 0.8 μm. Measured f_t for other devices with gate lengths of 1.1 and 0.7 μm on this wafer were 15.4 GHz and 22.5 GHz respectively. The effective saturated velocity in the channel estimated from the slope of the f_t vs 1/ L_g measured on several devices is 0.9-1.0 x 10^7 cm/s.

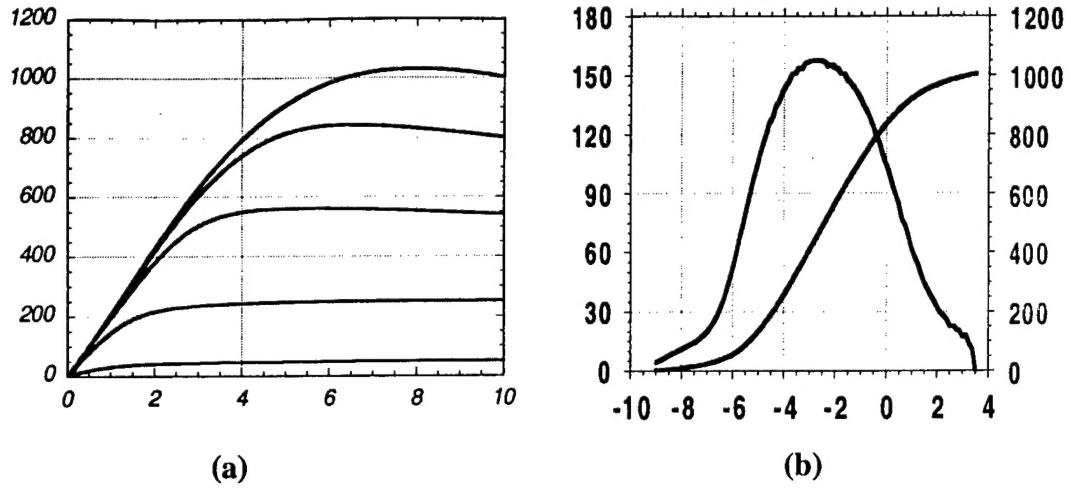

(a) (b)

Fig. 5.(a) *DC I-V characteristic showing maximum current in excess of 1 A/mm. (L_g = 0.6 μm, L_{ds} = 2.1 μm) V_{gs}: start = +2V, step = -2V*

Fig. 5 (b) *DC I-V characteristic peak transconductance of 160 mS/mm. (L_g = 0.6 μ m, L_{ds} = 2.1 μm) V_{gs}: start = 2V, step = -2V*

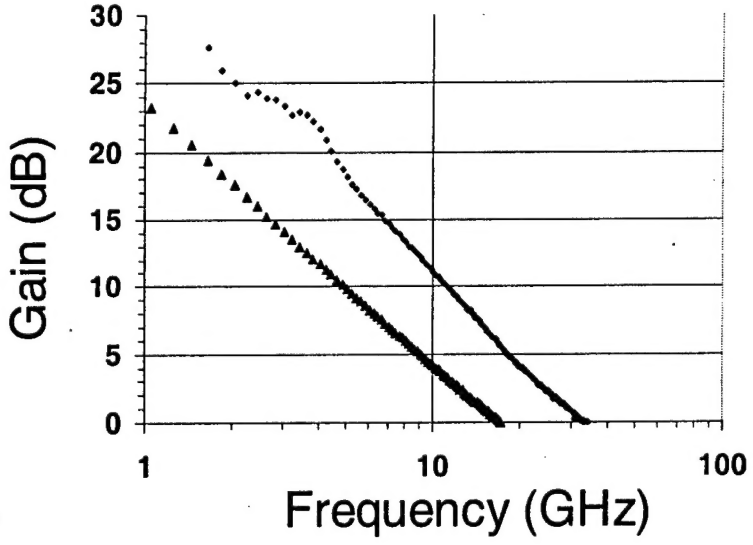

Fig 6. *Small signal performance*

Device dimensions: Lg = 0.8 μm, Lgd=1.4 μm, W = 150 μm. D.C. Bias V_{DS} = 9.0 V, f_t = 17.5 GHz and f_{max} = 33 GHz

On wafer, CW, large signal power measurements were performed at 6 GHz using an ATN Load Pull system. In all measurements, the wafer was resting on an uncooled metal chuck. The output power was measured at the fundamental frequency. On most devices, maximum output power exceeded 3.3 W/mm. Fig. 7 shows measured output power, large signal gain and power added efficiency (PAE) for a device with L_g = 0.8 μm, L_{gs} = 0.7 μm, L_{gd} = 1 μm and gate width of 150 μm. The device was biased at 26 V and 200 mA/mm. Maximum output power was_3.55 W/mm at an associated gain of 5.4 dB. The small signal gain was 14 dB and maximum PAE was 33.5%. These results are the highest reported output power density for MBE grown GaN HFETs and rival the best reported power performance of MOCVD grown GaN HFETs on sapphire substrates

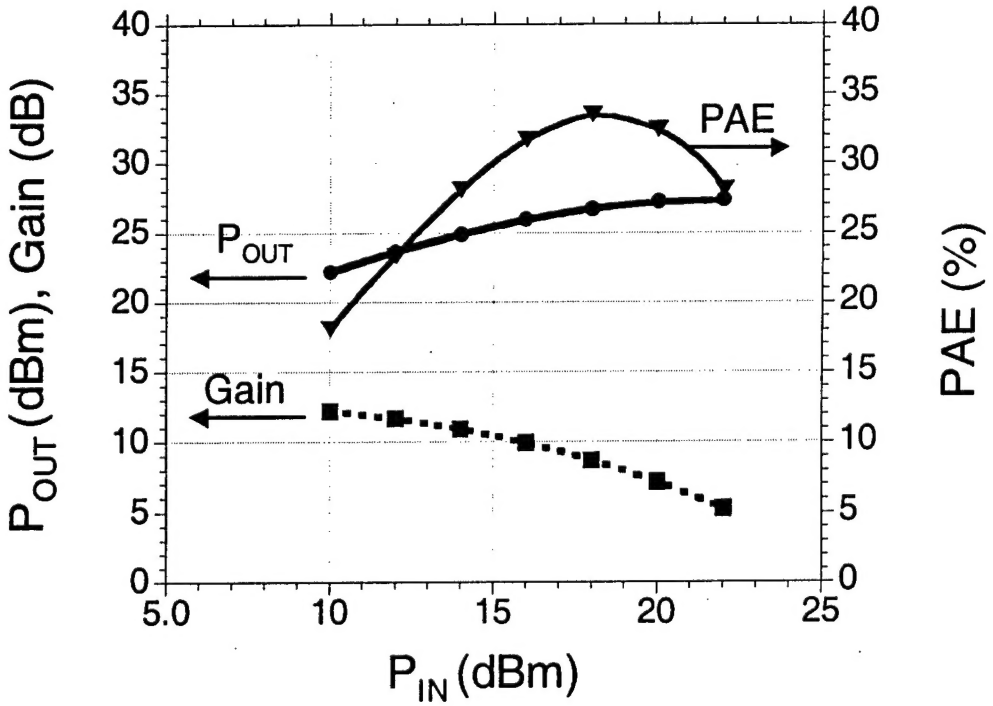

Fig 7. *Power performance at 6 GHz.*

Device dimensions: Lg = 0.8 μm, Lgd=1.4 μm, W = 150 μm. D.C. Bias VDS = 26V, IDS = 200 mA/mm. Maximum POUT = 27.3 dBm (3.55 W/mm) maximum PAE = 33.5%.

The results of this work are summarized in the papers listed below. The data have also been presented at several national and international conferences.

1. I.P.Smorchkova, C.R.Elsass, J.P.Ibbetson, R.Vetury, B.Heying, P.Fini, E.Haus, S.P.DenBaars, J.S.Speck and U.K.Mishra "Polarization-induced charge and electron mobility in AlGaN/GaN heterostructures grown by plasma-assisted molecular-beam epitaxy", *J.Appl.Phys.* (in press)

2. C.R.Elsass, I.P.Smorchkova, B.Heying, E.Haus, P.Fini, K.Maranowski, J.P.Ibbetson, S.Keller, P.M.Petroff, S.P.DenBaars, U.K.Mishra and J.S.Speck " High mobility two-dimensional electron gas in AlGaN/GaN heterostructures grown by plasma-assisted molecular beam epitaxy", *Appl.Phys.Lett.*, **74**, 3528 (1999)

3. B.Heying, C.Elsass, I.Smorchkova, T.Mates, E.Haus, P.Fini, S.P.DenBaars, U.Mishra, J.S.Speck "Record high mobility AlGaN/GaN heterostructures based on optimization of GaN by MBE", The 3rd International Conference on Nitride Semiconductors ICNS3, July 4-9, 1999, Montpellier, France

4. Chris R.Elsass, Yulia Smorchkova, Erik Haus, Paul Fini, Pierre Petroff, Steven P.DenBaars, Umesh Mishra, James Speck, Ben Heying " High Electron Mobility 2DEG in AlGaN/GaN Structures", 41st Electronic Materials Conference, June 30-July 2, 1999, Santa Barbara, CA

Heavy Doping Effects in Mg-doped GaN

The electrical properties of p-type Mg-doped GaN are investigated through variable-temperature Hall effect measurements. Samples with a range of Mg-doping concentrations were prepared by metalorganic chemical vapor phase deposition, and the Hall measurements were performed in conjunction with William Mitchel and Adam Saxler at Wright-Patterson Air Force Base. A number of phenomena are observed as the dopant density is increased to the high values typically used in device applications: the effective acceptor energy depth decreases from 190 meV to 112 meV, impurity conduction at low temperature becomes more prominent, the compensation ratio increases, and the valence band mobility drops sharply. The measured doping efficiency drops in samples with Mg concentration above 2×10^{20} cm^{-3}.

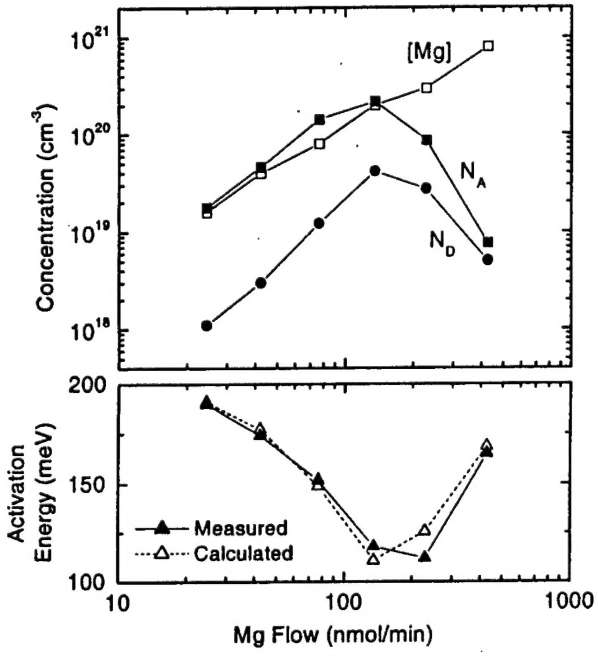

Figure: Concentration data extracted from the Hall effect and SIMS measurements are presented in the top plot. In the lower plot, the solid triangles represent the measured activation energy of the Mg dopant. The open triangles are calculated from the concentration data using a simple model to account for the activation energy reduction due to Coulomb interactions.

Paper submitted to Applied Physics Letters:

Peter Kozodoy, Huili Xing, Steven P. DenBaars, Umesh K. Mishra, A. W. Saxler, R. Perrin, S. Elhamri, W. C. Mitchel. "Heavy doping effects in Mg-doped GaN."

AFOSR [F49620-96-1-0398]
"Uncooled RF Electronics for Airborne Radar"

PUBLICATION LIST

P. Kozodoy, H. Xing, S.P. Denbaars, U.K. Mishra, A.W. Saxler, R. Perrin, S. Elhamri, W.C. Mitchel, "Heavy doping effects in Mg-doped GaN" J. Appl. Phys. 87(4), 1832-35 (2000).

I.P. Smorchkova, E. Haus, B. Heying, P. Kozodoy. P. Fini, J.P. Ibbetson, S. Keller, S.P. DenBaars, J.S. Speck, and U.K. Mishra, "Mg doping of GaN layers grown by plasma-assisted molecular-beam epitaxy" Appl. Phys. Lett. 76(6), 718-20 (2000).

R. Vetury, I.P. Smorchkova, C.R. Elsass, B. Heying, S. Keller, and U.K. Mishra, "Polarization induced 2DEG in MBE grown AlGaN/GaN HFETs: On the origin, DC and RF characterization" Mat. Res. Soc. Symp. Vol. 622 © 2000 Materials Research Society.

G. Parish, S. Keller, P. Kozodoy, J.P. Ibbetson, H. Marchand, P.T. Fini, S.B. Fleischer, S.P. DenBaars, U.K. Mishra and E.J. Tarsa, "High-performance (Al,Ga)N-based solar-blind ultraviolet p-i-n detectors on laterally epitaxially overgrown GaN" Appl. Phys. Lett. 75(2), 247-9 (1999).

S. Keller, G. Parish, P.T. Fini, S. Heikman, C.-H. Chen, N. Zhang, S.P. DenBaars and U.K. Mishra, "Metalorganic chemical vapor deposition of high mobility AlGaN/GaN heterostructures" J. Appl. Phys. 86(10), 5850-7 (1999).

I.P. Smorchkova, C.R. Elsass, J.P. Ibbetson, R. Vetury, B. Heying, P. Fini, E. Haus, S.P. DenBaars, J.S. Speck, U.K. Mishra, "Polarization-induced charge and electron mobility in AlGaN/GaN heterostructures grown by plasma-assisted molecular-beam epitaxy" J. Appl. Phys. 86(8), 4520-26 (1999).

G. Parish, S. Keller, P.T. Fini, R. Vetury, C.-H. Chen, S.P. DenBaars, U.K. Mishra and Y.-F. Wu, "MOCVD growth and properties of thin AlxGa1-xN layers on GaN" Proc. IEEE COMMAD Perth, Australia, 478-81 (1998).

G. Parish, S. Keller, P. Kozodoy, J.P. Ibbetson, H. Marchand, P.T. Fini, S.B. Fleischer, S.P. DenBaars, U.K. Mishra and E.J. Tarsa, "Low dark current p-i-n (Al,Ga)N-based solar-blind UV detectors on laterally epitaxially overgrown GaN" Proc. IEEE COMMAD Perth, Australia, 175-8 (1998).

PATENTS

UC CASE #	*INVENTORS*	*INVENTION TITLE*
97-195-2	Mishra/Keller, S./ Keller, B./DenBaars	"Insulating GaN'